RADIOCARBON PROTOCOLS AND FIRST INTERCOMPARISON RESULTS FROM THE CHRONOS [14]CARBON-CYCLE FACILITY, UNIVERSITY OF NEW SOUTH WALES, SYDNEY, AUSTRALIA

Chris Turney[1,2,3*] • Lorena Becerra-Valdivia[1,2,3*] • Adam Sookdeo[3,4*] •
Zoë A Thomas[1,2,3] • Jonathan Palmer[1,2,3] • Heather A Haines[1,2,3] • Haidee Cadd[1,2,3] •
Lukas Wacker[5] • Andy Baker[2,3] • Martin S Andersen[6] • Geraldine Jacobsen[7] •
Karina Meredith[7] • Khorshed Chinu[4] • Silvia Bollhalder[5] • Christopher Marjo[1,2,4]

[1]Chronos [14]Carbon-Cycle Facility, Mark Wainwright Analytical Centre, University of New South Wales, Sydney, NSW 2052, Australia
[2]Earth and Sustainability Science Research Centre (ESSRC), School of Biological, Earth and Environmental Sciences, University of New South Wales, Sydney, NSW 2052, Australia
[3]Australian Research Centre of Excellence in Australian Biodiversity and Heritage (CABAH), University of New South Wales, Sydney, NSW 2052, Australia
[4]Mark Wainwright Analytical Centre, University of New South Wales, Sydney, NSW 2052, Australia
[5]Laboratory of Ion Beam Physics, ETH Zurich, HPK, H29, Otto-Stern-Weg 5, CH-8093 Zürich, Switzerland
[6]School of Civil and Environmental Engineering, University of New South Wales, Sydney, NSW 2052, Australia
[7]Australian Nuclear Science and Technology Organisation (ANSTO), New Illawarra Road, Lucas Heights, NSW 2234, Australia

ABSTRACT. The Chronos [14]Carbon-Cycle Facility is a new radiocarbon laboratory at the University of New South Wales, Australia. Built around an Ionplus 200 kV MIni-CArbon DAting System (MICADAS) Accelerator Mass Spectrometer (AMS) installed in October 2019, the facility was established to address major challenges in the Earth, Environmental and Archaeological sciences. Here we report an overview of the Chronos facility, the pretreatment methods currently employed (bones, carbonates, peat, pollen, charcoal, and wood) and results of radiocarbon and stable isotope measurements undertaken on a wide range of sample types. Measurements on international standards, known-age and blank samples demonstrate the facility is capable of measuring ^{14}C samples from the Anthropocene back to nearly 50,000 years ago. Future work will focus on improving our understanding of the Earth system and managing resources in a future warmer world.

KEYWORDS: archaeological science, climate-carbon cycle dynamics, earth science, earth system science, radiocarbon calibration.

INTRODUCTION

The Chronos [14]Carbon-Cycle Facility (henceforth Chronos) is a new dedicated radiocarbon (^{14}C) and stable isotope facility established at the University of New South Wales, Sydney (UNSW), in collaboration with the Australian Nuclear Science and Technology Organisation (ANSTO). UNSW had previously been home to a radiocarbon laboratory in the School of Chemistry (spanning 1960s to 1986) (Southwell-Keely 2020), but Chronos has been established as a cross-faculty facility housed in a new laboratory space within the Science and Engineering Building, as part of the Mark Wainwright Analytical Centre (MWAC). Funded through the UNSW *2025 Strategic Plan*, the aim of this facility is to provide greater radiocarbon research capacity for the Earth, Environmental and Archaeological sciences.

As the planet faces unprecedented rates of global environmental and societal change in the Anthropocene, there is an urgent need to improve our understanding of the Earth System (Lewis and Maslin 2015; Steffen et al. 2015, 2018). A key source of uncertainty over the timing and impacts of future change is that historical (instrumental) records of change are too short (since CE 1800) and their amplitude too small relative to projections for the next

*Corresponding authors. Emails: c.turney@unsw.edu.au; Lorena.becerravaldivia@arch.ox.ac.uk; a.sookdeo@unsw.edu.au

century (IPCC 2018), raising concerns over our ability to successfully plan for future change. Growing populations threaten to erode the sustainable use of the global resource base, including water resources, with substantial economic implications. In Australia alone, groundwater supplies support manufacturing, agriculture, and mining worth $34 billion/year, but are facing increasing exploitation (Deloitte Access Economics 2013). Future climate extremes are likely to increase in amplitude and frequency compared to the historic period, enhanced by climate-human-carbon feedbacks (Friedlingstein et al. 2013; Le Quéré et al. 2013; Bradford et al. 2016; Graham et al. 2015; Randerson et al. 2015; Fu et al. 2020; McDonough et al. 2020). Such changes could have substantial and irreversible consequences for Australia's (and the world's) climate and environment.

Detailed radiocarbon analyses of Earth, environmental, and archaeological records have considerable potential for providing insights into the mechanisms and impacts of regional and global change that pre-date the observational period (Thomas 2016; Dougherty et al. 2019; Reimer et al. 2020; Rockman and Hritz 2020; Steffen et al. 2020). A wealth of "natural archives" (or "palaeo archives," such as tree rings, lake sediments, speleothems, and ice cores) are available to extend instrumental records of environmental change. In combination with increasingly detailed archaeological analyses, records of past change offer an improved understanding of environmental variability and impacts in the Earth system but require the development of accurate age models for precise comparison. For instance, past extreme and rapid climate changes are now widely recognized in numerous natural archives and appear to be associated with substantial disruptions in the global carbon cycle (Treble et al. 2017; Steffen et al. 2018; Fogwill et al. 2020). These major environmental changes are often paralleled by patterns of past human migration and adaptation (Turney and Hobbs 2006; Zhang et al. 2011; O'Connell et al. 2018; Becerra-Valdivia and Higham 2020; Douglass and Cooper 2020).

To better understand contemporary processes in the Earth system, there is an increased demand for a wide range of radiocarbon applications. An expanded network of annually-resolved tree-ring records in regions where there is currently a dearth of datasets (e.g., the tropics and subantarctics) (Brienen et al. 2016; Haines et al. 2018; Hogg et al. 2020) offers the opportunity to reduce the uncertainty surrounding contemporary and projected multidecadal to subannual carbon-climate dynamics (Friedlingstein et al. 2019; Varney et al. 2020). In the subsurface, radiocarbon can provide insights into the sources and sinks of organic carbon in drinking water treatment (Bridgeman et al. 2014), understanding the source of river evaded carbon dioxide (Billett et al. 2007), and determining the age and source of labile aquatic organic matter in natural and urban systems (Hedges et al. 1986; McDonough et al. 2020). Along with partners ANSTO, the new facility enhances capacity for these analyses and aims to address these global questions by increasing the number of ^{14}C measurements available to the scientific community. This was the primary motivation for the establishment of the Chronos facility.

INSTRUMENTS

The centrepiece of the Chronos facility is a 200 kV MIni-CArbon DAting System (MICADAS) Accelerator Mass Spectrometer. The first prototype of MICADAS was developed in 2007 integrating a unique low energy (200 kV), vacuum insulated acceleration unit at the Laboratory of Ion Beam Physics, ETH, Zurich (Synal et al. 2007; Wacker et al. 2010a), and subsequently built and distributed by Ionplus. The MICADAS systems are now found

Figure 1 The Chronos [14]Carbon-Cycle Facility at the University of New South Wales. Panel A: Elemental analyzer with Carbonate Handling System 2 and Automated Graphitisation Equipment 3. Panel B: The MIni-CArbon DAting System (MICADAS) with New Zealand ancient kauri workstation at the University of New South Wales. Panel C: Elemental analyzer coupled to an isotope ratio mass spectrometer with the Gas Interface System.

in numerous institutions around the world (Kromer et al. 2013; Bard et al. 2015; Knowles et al. 2019). In October 2019, a MICADAS was installed in the Chronos Facility. This is the 25th system in operation and the first to be located in the Southern Hemisphere. Chronos also includes a gas interface system for the direct injection of CO_2 into the MICADAS (Gas Interface System or "GIS," Ionplus) (Wacker et al. 2013a), a cracker for gas samples sealed in glass tubes (Tube Sealing Equipment or "TSE," Ionplus), three Elementar vario ISOTOPE cube elemental analyzers (EA) for sample combustion, an automated system to handle carbonates using wet chemistry (Carbonate Handling System 2 or "CHS2," Ionplus), an automated graphitization system (Automated Graphitization Equipment 3 or "AGE3," Ionplus), and an EA-coupled Elementar precisION® isotope ratio mass spectrometer (IRMS) (Figure 1).

SAMPLE PREPARATION METHODS

The Chronos Facility is capable of handling a wide range of sample material types. Here we outline the sample preparation methods of the material types that have formed the focus for the facility during the first year of operation: wood, bone, carbonates, charcoal, peat, and pollen. The following describes the rational for selecting suitable samples for ^{14}C analysis and subsequent processing at the Chronos facility.

Sampling

For bone and shell samples, where possible, the surfaces are cleaned by air abrasion with aluminium oxide powder to remove superficial contaminants. Bone fragments are then cut manually or using a small diamond disc, and both bone and carbonate (shell) samples are crushed with a pestle and mortar (stainless steel) prior to processing. For bone collagen pre-screening (see section below), sampling is undertaken by drilling with a cleaned tungsten carbide spherical burr drill bit. Here we follow DeNiro and Weiner (1988) in their use of the term "collagen."

For peat and lake sediments, terrestrial macrofossils are generally considered to be the most reliable material for ^{14}C sample selection within a sediment matrix (Lowe and Walker 2000; Bronk Ramsey et al. 2012; Thomas et al. 2019). Terrestrial macrofossils are carefully selected with tweezers and cleaned of surrounding sediment (under a low-power microscope if necessary). Fruits, leaves, stems, twigs, and branches are all suitable material, with dry weights of >3 mg. It is vital that roots or rootlets are removed to prevent contamination through the intrusion of younger carbon from overlying sediments. If terrestrial macrofossils cannot be identified, the humin or humic fraction from bulk peat/sediment samples is measured instead, though these fractions may be more vulnerable to contamination (Walker et al. 2012; Strunk et al. 2020). If bulk peat/sediment is analyzed, care is taken to remove any roots prior to chemical pretreatment. If bulk sediment is not desirable or considered appropriate for a sequence, terrestrial microfossils, such as pollen, are targeted for dating (Brown et al. 1992; Vandergoes and Prior 2003; Howarth et al. 2013; Tennant et al. 2013). Pollen concentrates are extracted from bulk peat/sediment samples using modified palynological methodologies (Bennett and Willis 2002). If the pollen concentrations of bulk sediment samples are unknown, preliminary sample processing is performed to determine the sample quantity required (see below).

For tree rings, if tree cores are glued to core mounts, the wood is removed using a scalpel and then placed in acetone for 1–2 hr so that the glue becomes malleable and can be wiped from the core. Should any glue remain after this, a scalpel is used to cut the remaining glue from the core. Once a wood sample is dry, one of two methods is employed. For annual ^{14}C measurement of tree rings, each ring is carefully cut from the sample using a scalpel. Care is taken to ensure that the sample does not extend beyond the selected ring boundaries. The annual ring is then cut into small, thin rectangular pieces ("matchsticks") being certain that each piece spans the entire year's growth (>10 mg although 50 mg is desirable depending on the age and condition of the sample). For multi-year dating (e.g., decadal-block samples), the ring boundaries bracketing the desired period are carefully sampled to make sure no growth extends beyond these rings.

Chemical Pretreatment

Routine pretreatment methods at Chronos are identified with unique pretreatment (P) codes. These differ according to each material type, the sources of contamination, the degree of preservation, and are assigned following due assessment. If solvent is used to remove contaminants (e.g., glue on bone or wood) prior to pretreatment, the code is followed by an asterisk (e.g., UFC* or BABAB*). Samples are pretreated in batches of 16–28, depending on the material type. With every batch, we undertake at least one duplicate sample that undergoes separate chemical pretreatment for further quality control. Matrix-matched, known-age samples are included in each chemical pretreatment batch for background subtraction calculations and/or as quality assurance checks (Table 1). Following pretreatment, all samples are lyophilized (AdVantage Pro XL, SP Scientific). Glassware and equipment within Chronos are solely dedicated to radiocarbon dating. Prior to use, glassware is washed and baked in a 500ºC oven for 3 hr to reduce carbon contamination.

Bone

To assess bone collagen preservation, samples might be first pre-screened for nitrogen content following Brock et al. (2010a). Nitrogen content is a suitable proxy for collagen preservation as it derives exclusively from the protein component in bone (Sillen and Parkington 1996). This method involves measuring the weight % N of 1 mg of whole bone powder with a CN elemental analyzer (vario ISOTOPE select, Elementar). Acetanilide (Sigma-Aldrich) is used as a standard.

For bone samples with conservation-derived contamination, solvent extraction precedes routine pretreatment. If the contaminant is known, e.g., shellac, tailored protocols following Brock et al. (2018) are employed. Otherwise, samples are sequentially washed with acetone (30–60 min, 40ºC), methanol (30–60 min, 40ºC), and chloroform (30–60 min, at room temperature or "RT") (Brock et al. 2010b) and left to dry.

Routine pretreatment involves acid-base-acid (ABA) immersions, gelatinization (Longin 1971), filtration, and ultrafiltration (Brown et al. 1988) (pretreatment code "UFC"). If the sample is believed or shown to be poorly preserved, however, ultrafiltration is omitted (pretreatment code "SFC"). Depending on the bone sample and its degree of contamination, a SFC date should only be viewed as a *terminus ante quem*.

Sequentially, bone samples are placed in 0.5 M hydrochloric acid (3-4 rinses every 2 hr and overnight for approximately 20 hr; RT), 0.1 M sodium hydroxide (30 min; RT), and 0.5 M hydrochloric acid (1 hr; RT), with 3 rinses of Milli-Q® water between each reagent. Separation is either through decanting or glass pipetting (these are baked for 3 hr at 500ºC prior to use) and is typically aided by centrifugation. The crude collagen is then gelatinized in pH 3 solution at 75ºC for 20 hr, and the resulting gelatin is filtered using non-sterile syringe filters (Millex, Durapore®; 45 μm pore size). These are cleaned by flushing with 10 mL of Milli-Q® water, followed by 10 mL of 0.5 M HCl, and finally once more with 10 mL of Milli-Q® water. The syringe-filtered gelatin is then decanted into an ultrafilter (Sartorius™ Vivaspin™ Turbo 15, 30 kD MWCO, polyethersulfone membrane) and centrifuged at 2550 rpm until 0.5–1.0 mL of the >30 kD fraction remains. Ultrafilters are cleaned using Milli-Q® water by rinsing, centrifuging at 2550 rpm for 10 min twice, ultrasonication for 1 hr, soaking overnight, a further three centrifugations, and a final rinse. After the fourth centrifugation, a sample of the Milli-Q® water in the ultrafilter is

Table 1   Known-age and background samples used at the Chronos facility.

Material	Sample	Location	Age or $F^{14}C \pm 1\sigma$
Bone collagen	Mammoth longbone ("Hollis mammoth")	Yukon, Canada	0.0031 ± 0.0002[a]
	Cow longbone (from 1841 *William Salthouse* shipwreck)	*William Salthouse* shipwreck, Port Philip Bay, Victoria, Australia	CE 1841 (*terminus ante quem*)[b]
Carbonate	IAEA C1	Carrara, Italy	Mesozoic[c]
Charcoal	Ancient kauri (*Agathis australis*) charcoal*	Manukau (Renton Road), New Zealand	Marine Isotope Stage 7 (>140,000 yrs) with reported $F^{14}C$ of 0.000707 ± 0.00003[d]
Charcoal	Ancient kauri (*Agathis australis*) charcoal*	Towai, New Zealand	0.2742 ± 0.0004[e]
Oxalic acid	NIST OxA2 (SRM 4990C)		1.3407 ± 0.0005[f]
Oxalic acid	IAEA-C8		0.1503 ± 0.0017[g]
Peat	Peat	Thirlmere Lakes, Australia	Marine Isotope Stage 5 (130,000–80,000 yr)[h]
Pollen	Extracted from peat bed	Tussac House peat deposit, Stanley, Falkland Islands	Early-Mid Pliocene (~5.3–3 million yr)[i]
Wood	Ancient kauri (*Agathis australis*) wood	Manukau (Renton Road), New Zealand	Marine Isotope Stage 7 (>140,000 yr) with reported $F^{14}C$ of 0.000707 ± 0.00003[d]

*These wood samples were charred inside a sealed stainless-steel pyrolysis vessel at 450ºC for 4 hr (following drying at 150ºC for 1 hr). The pyrolysis vessel had been previously baked at 600ºC for 1 hr.

[a]De La Torre et al. (2019).

[b]Staniforth (1997).

[c]Dean (1988); Rozanski (1991).

[d]Hogg et al. (2006); Marra et al. (2006).

[e]Hogg et al. (2016a, 2016b).

[f]$F^{14}C$ value normalized to $\delta^{13}C$ value of –25‰ (Rasberry 1999; Bard et al. 2015).

[g]Le Clercq et al. (1997).

[h]Forbes et al. (2021).

[i]Unpublished site but preliminary work suggests correlation to Forest Bed at West Point, Falkland Islands (Macphail and Cantrill 2006).

collected and tested for wt% C as a quality control using an EA. Finally, the ultrafiltered gelatin is transferred into a test tube using clean glass pipettes to be lyophilized.

Carbonates
If carbonate samples are too fragile for shot blasting, these are placed inside exetainers (Exetainer®, Labco) and depending on the sample size, leached using the necessary amount of 0.1 M HCl to remove secondary carbonates in the outer layer (10–20% for foraminifera and coral, and 40–50% for shell; pretreatment code "LC") (Wacker et al. 2013b). The samples are then washed with Milli-Q® water twice and dried in a heating block prior to processing. If no leaching is performed, the pretreatment code assigned is "CC."

Charred/Non-Charred Plant Remains
Routine protocols for charred and non-charred plant remains involve standard ABA pretreatment (pretreatment codes "CP" and "NCP", respectively). First, acid-soluble organic matter and carbonates are removed with a 1 M HCl wash (20 min at 80°C), followed by three Milli-Q® water rinses. Acid insoluble organic matter is then removed with a 0.2 M NaOH wash (20 min at 80°C). This step is repeated until the solution is nearly colorless to ensure complete aromatic organic matter removal. This is again followed by three Milli-Q® water rinses. Pretreatment is completed by a third wash, an immersion in 1 M HCl for 1 hr at 80ºC, three subsequent Milli-Q® water rinses, then lyophilization. This last step removes any base-liberated acid-soluble organic matter and atmospheric CO_2 absorbed during the same wash. Small or very fragile materials are treated with 1 M HCl at RT for 1 hr and sonicated for 15 min (optional) prior to three Milli-Q® water rinses and then lyophilized (pretreatment code "FP").

Peat/Sediment
Where extraction of macrofossils within a sediment matrix is not possible, and/or if peat is highly humified, it is possible to date a bulk "humin" or "humic" (aqueous alkaline-extractable) acid fraction. For samples containing significant sand or large fragments (such as root material), wet sieving at 125–250 μm, prior to pretreatment, may be necessary. For clay-rich or dense sediment, sonication in Milli-Q® water prior to pretreatment may be necessary. Routine protocol for a bulk "humin" fraction involves a slightly modified standard ABA pretreatment (pretreatment code "PS").

Acid soluble organic matter and carbonates are removed from sediment samples with a 1 M HCl wash (20 min at 80°C). Samples are gently mixed with a vortex mixer after any initial reaction has ceased. HCl treatment is followed by three Milli-Q® water rinses. Alkaline-soluble organic matter is removed with a 0.2 M NaOH wash (20 min at 80°C). Samples are mixed with a vortex mixer prior to heating. This step is repeated until the solution is nearly colorless to ensure complete chromophoric organic matter removal. For highly humified samples, the NaOH step should only be completed until highly labile, potentially foreign sorbed organic matter has been removed. Following the final NaOH wash, samples are rinsed in Milli-Q® water three times. Samples are then immersed and mixed with a vortex mixer in 1 M HCl for up to 1 hr at 80ºC and rinsed three times with Milli-Q® water. This last step removes any base-liberated fulvic acids and atmospheric CO_2 absorbed during the NaOH wash. The samples are first frozen, then lyophilized.

If the alkaline-soluble organic matter fraction ("humic acid") is to be dated (pretreatment code "HA"), the same steps above are followed, but the NaOH supernatant is decanted into a separate beaker rather than discarded. Excess 4 M HCl is added to the NaOH solution and heated for up to 1 hr. The resulting precipitate, an alkali soluble and acid insoluble fraction, is the humic fraction. The solids are subsequently rinsed three times in Milli-Q® water to remove trace fulvic acids and residual salts from the precipitation step.

Pollen

Where extraction of macrofossils within a sediment matrix is not possible and the use of the bulk fraction is considered undesirable, terrestrial microfossils, such as pollen, can be extracted from sediment for radiocarbon dating (pretreatment code "POL"). Samples are thoroughly mixed with a vortex mixer between each rinse during pretreatment. For clay-rich or dense sediment, sonication in Milli-Q® water prior to pretreatment may be necessary. For samples containing significant sand or large fragments wet sieving at 125–250 μm, prior to pretreatment, may be necessary.

Firstly, alkaline-soluble organic matter is removed with a 1 M NaOH wash (20 min at 80ºC). This step is repeated until the solution is nearly colorless to ensure complete humic acid removal. Samples are rinsed three times in Milli-Q® water following the final NaOH wash. Silicate and inorganic particles are removed from samples via a series of sieving and density separation steps until sufficient pollen concentrates are achieved. Samples are dispersed in Milli-Q® water and gently sieved through a 100 μm pluriStrainer. After excess water is decanted, 6 mL of sodium polytungstate (SPT) of 1.8 g cm^{-3} density is added to each sample and thoroughly agitated. Samples are centrifuged at 2200 rpm for 25 min to allow effective separation of organic and inorganic particles. After centrifugation, the base of each sample tube is immersed in liquid nitrogen and the organic float decanted into clean centrifuge tubes and rinsed three times in Milli-Q® water. The float material is examined under a light microscope to check sample purity and concentration prior to additional sieving steps. If a target pollen type is to be isolated, samples are sieved to the identified pollen size range using 100, 70, 20, or 15 μm pluriStrainers. To remove fine organic and inorganic particles, samples are sieved through either a 10 or 5 μm pluriStrainer. Material captured in the sieve is rinsed from sieve mesh to a clean centrifuge tube with Milli-Q® water. Finally, samples are immersed in 1 M HCl for up to 1 hr at 80°C and rinsed three times with Milli-Q® water to remove any base-liberated and acid-soluble organic matter, and atmospheric CO_2 absorbed during pretreatment, then lyophilized.

Wood

The routine protocol for the chemical pretreatment of wood samples uses a five step base-acid-base-acid-bleaching (BABAB) procedure to extract cellulose (Němec et al. 2010; Sookdeo et al. 2020). The chemical procedures are performed at a temperature of 75°C using thinly sliced pieces of wood. These wood pieces are placed into a 5 mL of 1M NaOH, overnight. The sample is then rinsed twice with 10 mL Milli-Q® water before being placed into 5 mL of acid solution of 1.3M HCl for 30 min. Following two 10 mL Milli-Q® water rinses a second base wash of 5 mL of 1M NaOH for 1.5 hr is undertaken. The samples are then rinsed once with 10 mL Milli-Q® water then once with 5 mL acid (1.3M HCl). The pretreatment ends with a final bleaching wash of 5% NaClO$_2$ adjusted to pH 2 with HCl to remove lignin for 2–3 hr, depending on the nature of the wood sample. Once all lignin has visibly been removed, the samples are rinsed 2–3 times with 10 mL of Milli-Q® water before being lyophilized. Resin-rich wood samples, typical of subfossil wood that has been preserved in a wetland or bog setting, are treated for 30 min in

acetone at 55ºC followed by two 10 mL Milli-Q® water rinses. This helps remove the resin before beginning the BABAB treatment.

Elemental and Stable Isotope Analysis

Elemental and stable isotope analysis for carbon and nitrogen are determined using an Elementar precisION® isotope ratio mass spectrometer coupled to an Elementar vario ISOTOPE cube elemental analyzer. Stable carbon and nitrogen isotopic compositions are calibrated relative to the Vienna Pee Dee Belemnite (VPDB) and atmospheric N_2 (AIR) scales using international standards USGS40, USGS41, and USGS64. Measurement uncertainty is currently monitored using L-Alanine (Sigma-Aldrich) and homegrown broccoli (HBS) as internal standards with characterized isotopic compositions (n = 43, $\delta^{13}C$ = –19.08 ± 0.13‰, $\delta^{15}N$ = –1.64 ± 0.26‰, for the former, and n = 30, $\delta^{13}C$ = 31.02 ± 0.07‰, $\delta^{15}N$ = 5.22 ± 0.14‰, for the latter). We are in the process of characterizing two further internal standards: modern whale bone collagen and peat. Analytical uncertainty is calculated and reported following Szpak et al. (2017).

Graphitization

Samples are graphitized with an AGE3, which is described in detail elsewhere (Wacker et al. 2010c). Briefly, organic samples are weighed and placed into the EA sample holder where they are dropped one at a time into a heated chamber (>900ºC); oxygen gas is fed in for 50 s to facilitate the combustion of carbon to carbon dioxide. Using the CHS2, carbonate samples (inside exetainers) are flushed with helium gas and hydrolysed with orthophosphoric acid (1 mL 85% v/v) at 70ºC. Once CO_2 evolution has ceased, water is retained on a phosphorus pentoxide (Merck SICAPENT®) trap and the carbon transferred to the AGE3 in a helium stream. Within the AGE3, CO_2 is concentrated in a zeolite trap, which is heated to release the carbon into one of seven reaction chambers. To limit cross-contamination, which is less than 0.6‰ for the entire process mentioned above (Wacker et al. 2010c), two replicates of either samples, standards or blanks (termed "pre-conditions") are prepared. Pre-conditions are run through both EA- and CHS2-AGE3 systems when switching between materials of different ^{14}C content. Gas stored in ampoules is transferred to the AGE3 system manually by means of an ampoule cracker, water trap, vacuum lines, and liquid nitrogen. Graphitized samples are then transferred to clean aluminium cathodes (Ionplus) and compacted with a press (PSP). A second AGE3 system is housed at ANSTO to support high throughput of samples for graphitization.

SAMPLE MEASUREMENT

Radiocarbon measurement is carried out on the Ionplus MICADAS, which is described in detail elsewhere (Synal et al. 2007; Suter et al. 2010; Wacker et al. 2010a). Specifics of tuning parameters for a MICADAS are given in Wacker et al. (2010a) and are followed before loading a magazine. A magazine contains 39 positions, which are cycled through every 5 min during a measurement. Typically, a magazine comprises seven oxalic acids (OXII, NIST SRM 4990c) spaced throughout the magazine, 25 unknown-age samples, four matrix-matched blanks, two in-house graphitized chemical blanks (Phthalic Anhydride; PhA; SigmaAldrich, PN-320064-10 g) and one in-house graphitized IAEA-C8 standard (Oxalic Acid, 15.03 ± 0.07 pMC) (Le Clercq et al. 1997). Routine tuning results in standards having a current of 20–33 μA for $^{12}C^+$ ions collected in the high-energy Faraday

Table 2 ^{14}C weighted mean values obtained from background sample types at the Chronos [14]Carbon-Cycle Facility. The number in parentheses is the standard deviation calculated from *N* analyses. None of these samples have been blank-corrected.

Background samples	Measured $F^{14}C$	*N* analyses
IAEA-C1	0.00152 (0.00042)	9
Charcoal, Manukau kauri, NZ	0.00212 (0.00039)	5
Bone, Hollis Mammoth, Canada	0.00180 (0.00011)	5
Peat, Thirlmere, Australia	0.00258 (0.00027)	8
Pollen, Tussac House, Falkland Is.	0.00316 (0.00076)	5
Wood, Manukau kauri, NZ	0.00136 (0.00043)	21

cup, and ratios of $^{13}C/^{12}C$ between 1.08–1.09×10^{-2}. Under these parameters, a measurement is carried out until at least 0.5 million counts of ^{14}C are measured on OXII, with a high-precision measurement yielding >1 million counts and taking 2 to 3 days.

The ion source of the MICADAS is also capable of accepting CO_2 gas using the Gas Interface System (Ruff et al. 2010; Wacker et al. 2013a). This feature can be used to analyze microgram amounts of carbon (Haghipour et al. 2019), "Speed Dating" for rangefinder ages (Sookdeo et al. 2017), and jointly determine $\delta^{13}C$ and ^{14}C ages with an EA-IRMS-MICADAS coupling (McIntyre et al. 2017). The Chronos facility is equipped with a GIS and future testing is planned to integrate this form of measurement into our procedures.

DATA ASSESSMENT AND REPORTING

Before radiocarbon measurements are assessed, quality assurance parameters are used. For bone collagen, %C, %N, C:N, $\delta^{13}C$, $\delta^{15}N$, and collagen yield (%) values are monitored to help identify the presence of contaminants and/or degree of preservation following pretreatment (DeNiro 1985; Van Klinken 1999), as well as reservoir offsets.

All ^{14}C measurements issued by Chronos have a UNSW- laboratory code, followed by a unique number. In case of differences in processing and quality assurance, a letter suffix is added to the laboratory code. UNSW-A codes are measurements where the pretreatment chemistry has been carried out externally, UNSW-B codes refer to externally-produced targets or cathodes, UNSW-C codes refer to measurements with decreased precision, and UNSW-D codes denote measurements with a caution note in terms of accuracy. Data reduction is carried out using the software BATS (Wacker et al. 2010b). For relatively young samples, we currently report the age uncertainty generated from BATS, as is. In the future, we will reassess the maximum precision possible at Chronos.

RESULTS AND DISCUSSION

Blank and Known-Age Samples

To investigate facility performance, we report ^{14}C measurements during the first year of operation. A summary of Fraction Modern ($F^{14}C$) results for known-age materials, international standards and blanks processed, graphitized and measured at Chronos are reported in Tables 2 and 3. All were obtained from full-size (~1000 µg C) graphite samples. The background measurements are consistent with published and inferred ages and, for the

Table 3 ^{14}C weighted mean values obtained from reference and known-age sample types at the Chronos ^{14}Carbon-Cycle Facility. The number in parentheses for measured $F^{14}C$ is the standard deviation calculated from N analyses. Measurements are background-corrected using matching sample type (Table 2).

Standard samples	Reference $F^{14}C$	Measured $F^{14}C$	N analyses
NIST OxA2	1.3407 ± 0.0005	1.3406 (0.0020)	64
Towai charcoal, NZ	0.2742 ± 0.0004	0.2763 (0.0012)	3
IAEA-C8	0.1503 ± 0.0017	0.1504 (0.0006)	12
	Calendar age of shipwreck	Measured age	N analyses
William Salthouse bone, Australia	CE 1841	135 (9) BP or *CE 1832-1891 (46.6% probability)*	3
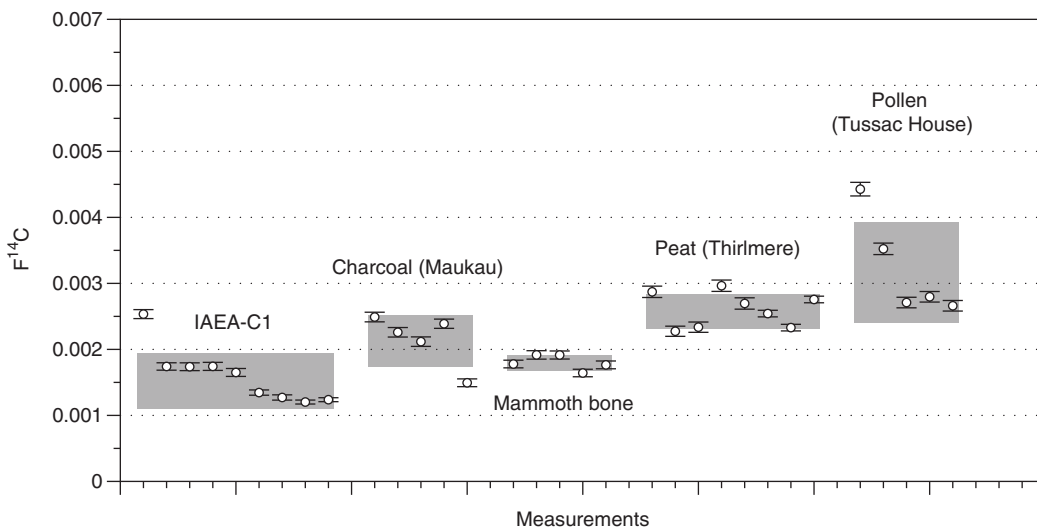
Figure 2   Radiocarbon measurements obtained from a range of blanks processed at Chronos. Gray bars are weighted-mean one standard deviation ranges obtained for the different sample types (Table 2).

former, show good agreement (Table 1). For instance, based on 9 targets, analysis of the IAEA carbonate standard, C1 (Mesozoic in age), we obtained a weighted average $F^{14}C$ of 0.0015 ± 0.0004. This is equivalent to a radiocarbon age of around 52,000 BP. Similarly, low $F^{14}C$ values have also been generated for the range of sample types being investigated at Chronos. This provides confidence that robust, finite ages <50,000 years can be obtained on bone, peat, pollen, charcoal and wood (Figure 2).

Importantly, previous work has reported a ^{14}C background (blank) value for the Marine Isotope Stage 7 Manukau kauri (New Zealand) of 0.00071 ± 0.00003 (Hogg et al. 2006). For Manukau kauri charcoal carbonized at Chronos (Table 1), we obtained a weighted mean of 0.0021 ± 0.0004 (Table 2), though it is important to note that the background
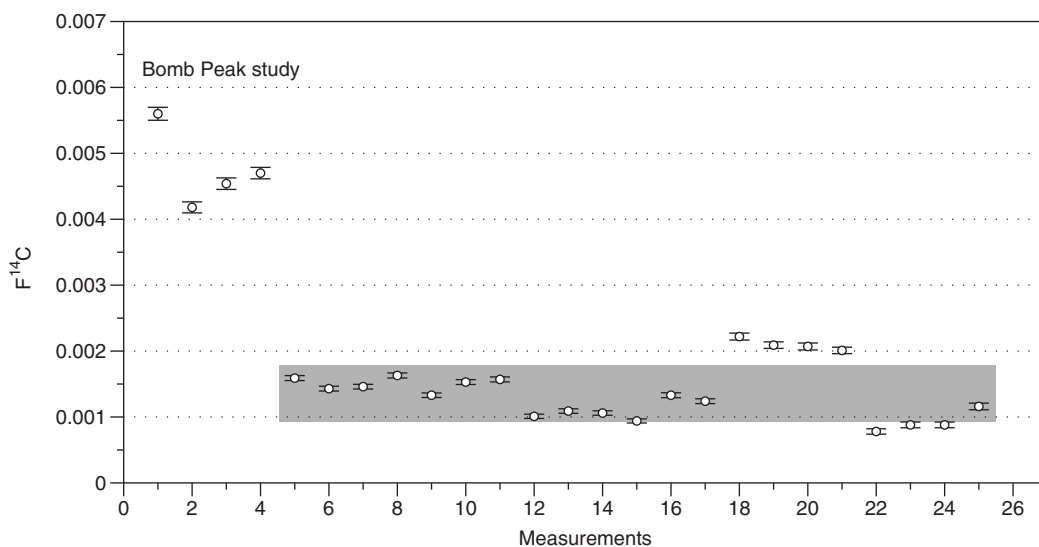
Figure 3   Radiocarbon measurements obtained from Ancient kauri (Marine Isotope Stage 7) cellulose blanks processed at Chronos. Ancient kauri from Manukau (Renton Road), New Zealand (Hogg et al. 2006; Marra et al. 2006). These blanks were used for the intercomparison studies (see text and Figure 5). The gray bar is the weighted-mean one standard deviation range obtained for measurements 5–25 (Table 2).

values were obtained by different methods (Hogg et al. 2006). We also investigated cellulose blanks, which formed the focus of our intercomparison study (see below). For the kauri cellulose, the $F^{14}C$ blanks obtained from magazine-to-magazine are <0.0022 ± 0.0004, except for measurements 1 to 4 (Figure 3), which were run for the "Bomb Peak" study (see below). The early blanks from measurements 1 to 4 were notably higher ($F^{14}C$ approximately 0.005), possibly due to residual contamination on the ion source following initial commissioning (Wacker et al. 2010a). However, these blank values had a minor influence on the uncertainty and accuracy for the "Bomb Peak" intercomparison study, given the enriched ^{14}C in the cellulose samples across this period ($F^{14}C>1.2$) (Turney et al. 2018). For the remaining 21 samples, we obtained a weighted mean of 0.0014 ± 0.0004, equivalent to a radiocarbon age of around 53,000 BP.

To confirm the accuracy and precision of the Chronos Facility, we measured reference oxalic samples (Table 3 and Figure 4). The NIST OxA2 (SRM 4990C) is used to correct and normalize measurements for the MICADAS AMS transmission and fractionation. The 64 analyses reported here provided a weighted mean $F^{14}C$ of 1.3406 with a standard deviation of 0.0020. The reported $F^{14}C$ value is 1.3407 ± 0.0005 (Rasberry 1999; Bard et al. 2015). Comparable levels of accuracy and precision were obtained for IAEA-C8, equivalent in age to approximately 15,200 BP. Here, we report 12 analyses, with a weighted mean $F^{14}C$ of 0.1504 and a standard deviation of 0.0006. The reported $F^{14}C$ value for IAEA-C8 is 0.1503 ± 0.0017 (Le Clercq et al. 1997).

To complement the above, we undertook measurements on a new internal standard for archaeological bone, a cow bone from the wreck of the *William Salthouse*, which was sunk at the entrance of Port Philip Bay as the vessel approached Melbourne in 1841 (Guiry et al. 2015). With a cargo of Canadian meat and fish, the cow bone provides a known historic age sample with a known (Northern Hemisphere) provenance. Following the
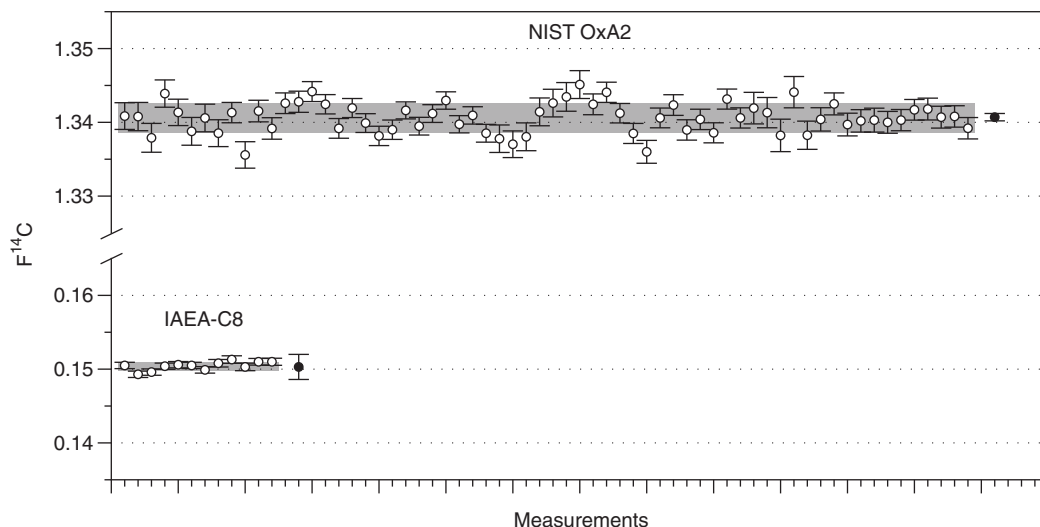
Figure 4   Radiocarbon measurements for the reference standards NIST OxA2 and IAEA-C8 processed at Chronos. The gray bars are the weighted-mean standard deviation range. The solid symbols are the reference mean and standard deviation values for OxA2 and C8 (Tables 1 and 3).
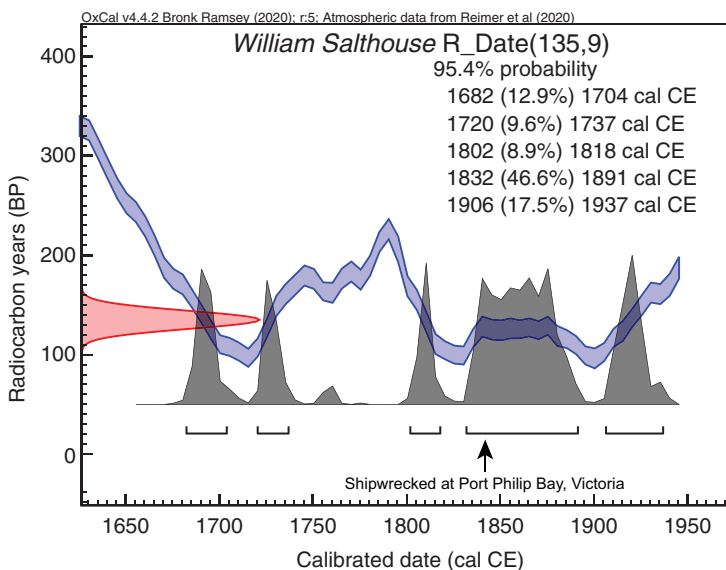

Figure 5   Calibration of Canadian cow bone from the 1841 *William Salthouse* shipwreck (Port Philip Bay, Victoria, Australia), an internal standard. Radiocarbon age calibration using IntCal20 (Reimer et al. 2020) and OxCal version 4.4 (Bronk Ramsey and Lee 2013).

processing protocols described above, we obtained a radiocarbon age of 135 ± 9 BP (n = 3; Table 3). We calibrated this age using IntCal20 but, because of the structure of the calibration curve during the eighteenth and nineteenth centuries, we obtained an age range of cal CE 1682–1937 (95.4% probability) (Figure 5). However, the calibrated age range

Table 4   Mean and standard deviation (1 σ) stable isotope and elemental values for Hollis Mammoth and the *William Salthouse* Shipwreck cow. %C and %N are the percentages of carbon and nitrogen in the combusted sample. C:N, atomic weight ratio of carbon to nitrogen. Stable isotope ratios are expressed in per mil (‰), relative to VPDB and atmospheric N_2 (AIR). The number in parentheses denotes the number of measurements used to generate weighted-average values.

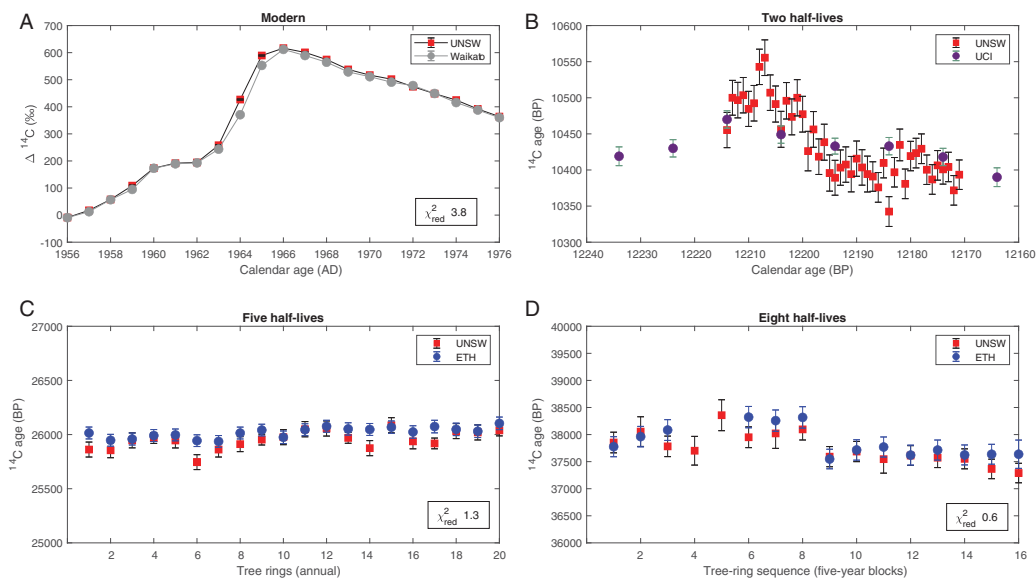| Standard name	C %	N %	C:N	$\delta^{13}C$, ‰	$\delta^{15}N$, ‰	Collagen yield %
Hollis Mammoth (n = 6)	43.7 ± 0.7	16.1 ± 0.3	3.2	−20.8 ± 0.1	6.8 ± 0.2	11.0 ± 0.5
William Salthouse shipwreck cow (n = 6)	43.2 ± 0.7	15.9 ± 0.3	3.2	−l20.7 ± 0.1	4.8 ± 0.1	10.3 ± 1.6

Figure 6 Intercomparison of tree ring ^{14}C measurements from selected time periods: (A) UNSW Δ^{14}C values (red) determined for the Bomb Peak ("Modern") samples of subantarctic *Dracophyllum scoparium* that were previously measured by the University of Waikato/UCI (gray) (Turney et al. 2017, 2018). (B) Annual ^{14}C ages obtained from New Zealand kauri (Towai) determined by UNSW (red) for a selected period within the Younger Dryas chronozone (approximately two half-lives), previously measured decadally by UCI (black) (Hogg et al. 2016a, 2016b; Palmer et al. 2016). (C) ^{14}C ages from Waipu kauri determined to be approximately 25,000 years old (approximately five half-lives) at UNSW (red) and ETH (blue). (D) ^{14}C ages determined for the Ngāwhā Springs approximately 40,000 years old (approximately eight half-lives) kauri samples at UNSW (red) and ETH (blue). Uncertainties are given as 1 σ.

with the greatest probability (46.6%) spans cal CE 1832–1891, consistent with the likely death of the cow within 1–2 years before the known date of the *William Salthouse* wreck (Guiry et al. 2015). In parallel with the radiocarbon results, stable isotope and elemental values for the *William Salthouse* shipwreck cow and the late Pleistocene Hollis Mammoth (Table 4) agree with previously published results (Guiry et al. 2015; De La Torre et al. 2019). Overall, our ^{14}C and stable isotope values validate the sample processing methods for a range of material types of different ages at the Chronos facility.

Intercomparison

Accuracy at Chronos was investigated by measuring a suite of contiguous tree-ring cellulose samples across selected time periods. Intercomparisons were carried out between the Chronos facility and three other institutes: the Swiss Federal Institute of Technology (ETH), University of California, Irvine (UCI), and the University of Waikato (Waikato) (Figure 6). Measurements and sample processing methods from UCI and Waikato are published by (Hogg et al. 2016a, 2016b) and (Turney et al. 2018), respectively. Chronos and ETH results are presented in this study. The ETH protocol for wood is similar to that described above and published previously (Sookdeo et al. 2020).

University of Waikato

Samples measured by Waikato covered the thermonuclear weapons testing period between CE 1956 to 1976 that created a peak in atmospheric ^{14}C. The so-called Bomb Peak resulted from anthropogenic stratosphere $^{14}CO_2$, that transferred down into the troposphere. Through the late Northern Hemisphere spring exchange of air masses, zonal mixing and meridional atmospheric circulation, bomb related-^{14}C was globally distributed (Dutta 2016). The resulting peak in atmospheric ^{14}C has been detected in tree-rings that grow on the remote subantarctic Campbell Island in the southwest Pacific (Turney et al. 2018). Here we focussed on an individual of *Dracophyllum scoparium*, one of a pair of related native tree species that are the most poleward growing in the southwest Pacific Ocean (Southern Ocean) and have been investigated as part of a previous study (Turney et al. 2017).

Our intercomparison results show an initial reduced χ^2 of 29 (n-1 = 20). Removing the largest laboratory offsets, which occurred between CE 1964–1965, the reduced χ^2 improves to 3.8 (n-1 = 18). It is likely that the offset across these two years of growth may be due to inconsistent tree-ring sampling in either this study or the previously published work (Turney et al. 2018). Around the time of the Bomb Peak, ring boundaries that may have been inadvertently incorporated into an adjoining growing season have the potential to skew the radiocarbon measurement (Turney et al. 2018); alternatively, given the rapid large changes in atmospheric ^{14}C, part of the growing season may have been missed. This is particularly true for the period 1964–1965, which experienced the steepest rise in atmospheric ^{14}C across the Bomb Peak and showed the largest laboratory offset (Figure 5a). Overall, however, the consistent values obtained from the two sets of analyses provides confidence that Chronos is capable of measuring twentieth century changes in atmospheric radiocarbon.

University of California, Irvine

We also undertook analyses on ancient kauri samples from Towai in Northland, New Zealand (35.5066˚S, 174.1729˚E), that span the Younger Dryas chronozone (Hogg et al. 2016a; Hogg et al. 2016b; Palmer et al. 2016). In the North Atlantic region, the Younger Dryas was characterized by a millennial-long cold period that started approximately 12,900 calendar years ago, accompanied by globally rising atmospheric CO_2 concentrations and warming across the mid- to high latitudes of the Southern Hemisphere (WAIS Divide Project Members 2015; Fogwill et al. 2020). The ^{14}C data measured at Chronos is sourced from the same tree as previously measured at UCI but subsampled at annual rather than decadal resolution. A χ^2 test was not conducted on these samples as the number of data points is insufficient (n-1=3). Annual ^{14}C data followed trends of the decadal measurements from UCI, particularly across the radiocarbon plateau, spanning 12,200–12,170 cal BP (Figure 5b). A depletion in atmospheric ^{14}C is evident in the annual ^{14}C data, which is not seen in the decadal ^{14}C measurements from UCI. This is interpreted as interannual variations captured in our record but averaged out in the decadal data from UCI.

Swiss Federal Institute of Technology (ETH)

As part of our intercomparison, two sets of kauri samples—the first set from five half-lives and the other from approximately eight half-lives ago—were analyzed at Chronos and ETH (Figure 5C and D, respectively). The first set was obtained from a tree excavated at Waipu, a site on the east coast in Northland (35.9517ºS, 174.4497ºE), and the second from Ngāwhā Springs, also in Northland (35.4027ºS, 173.8586ºE). As these samples did not have an

absolute calendar age, ^{14}C ages were plotted against consecutive sample numbers. The Chronos results show excellent agreement with ETH's results for both time periods.

The first set of intercomparison results from Waipu produced a reduced χ^2 of 1.3 (n = 20). The uncertainties are improved further when sample 1184, which had the largest laboratory offset, is removed. The second set of intercomparison results from Ngāwhā Springs produced a reduced χ^2 of 0.6 (n = 14), demonstrating a very good agreement of the datasets. The measured uncertainties may be considered relatively large not only because of the contribution of counting statistics (13–15‰) but also of the contribution of the estimated population uncertainty of cellulose blanks (±0.0004 in $F^{14}C$) (Sookdeo et al. 2020). Importantly, this reveals that samples such as these should be run in duplicate to better constrain ^{14}C uncertainties.

CONCLUSIONS

This paper reports the pretreatment methods, preliminary results, and reporting protocols for the new Chronos [14]Carbon-Cycle Facility, at the University of New South Wales. Built around an Ionplus 200 kV MIni-CArbon DAting System (MICADAS) AMS, the facility has now been operating since late 2019. In this time, we have been able to demonstrate radiocarbon and stable isotope measurements for a range of material types: bones, carbonates, peat, pollen, charcoal, and wood. A combination of international standards, samples of known-age, and blanks provides confidence in the Chronos Facility being capable of measuring ^{14}C samples from the Anthropocene to nearly 50,000 years ago. Future work will focus on refining these methods and exploring other sample types (e.g., dissolved inorganic and organic carbon in water) that are critical for improving our understanding of the Earth system and managing resources in a future warmer world.

ACKNOWLEDGMENTS

REFERENCES

Bard E, Tuna T, Fagault Y, Bonvalot L, Wacker L, Fahrni S, Synal H-A. 2015. AixMICADAS, the accelerator mass spectrometer dedicated to ^{14}C recently installed in Aix-en-Provence, France. Nuclear Instruments and Methods in Physics Research Section B: Beam Interactions with Materials and Atoms 361:80–86.

Becerra-Valdivia L, Higham T. 2020. The timing and effect of the earliest human arrivals in North America. Nature 584(7819):93–97.

Bennett KD, Willis KJ. 2002. Pollen. Tracking environmental change using lake sediments. Dordrecht, The Netherlands: Kluwer Academic Publishers. p. 5–32.

Billett MF, Garnett MH, Harvey F. 2007. UK peatland streams release old carbon dioxide to the atmosphere and young dissolved organic carbon to rivers. Geophysical Research Letters 34(23).

Bradford MA, Wieder WR, Bonan GB, Fierer N, Raymond PA, Crowther TW. 2016. Managing uncertainty in soil carbon feedbacks to climate change. Nature Climate Change 6(8):751–758.

Bridgeman J, Gulliver P, Roe J, Baker A. 2014. Carbon isotopic characterisation of dissolved organic matter during water treatment. Water Research 48:119–125.

Brienen RJ, Schöngart J, Zuidema PA. 2016. Tree rings in the tropics: Insights into the ecology and climate sensitivity of tropical trees. Tropical tree physiology. Springer. p. 439–461.

Brock F, Dee M, Hughes A, Snoeck C, Staff R, Ramsey CB. 2018. Testing the effectiveness of protocols for removal of common conservation treatments for radiocarbon dating. Radiocarbon 60(1):35–50.

Brock F, Higham T, Ditchfield P, Bronk Ramsey C. 2010a. Current pretreatment methods for AMS radiocarbon dating at the Oxford Radiocarbon Accelerator Unit (ORAU). Radiocarbon 52(1):103–112.

Brock F, Higham T, Ramsey CB. 2010b. Pre-screening techniques for identification of samples suitable for radiocarbon dating of poorly preserved bones. Journal of Archaeological Science 37(4):855–865.

Bronk Ramsey C, Lee S. 2013. Recent and planned developments of the program OxCal. Radiocarbon 55(2-3):720–730.

Bronk Ramsey C, Staff RA, Bryant CL, Brock F, Kitagawa H, van der Plicht J, Schlolaut G, Marshall MH, Brauer A, Lamb HF et al. 2012. A complete terrestrial radiocarbon record for 11.2 to 52.8 kyr B.P. Science 338(6105): 370–374.

Brown TA, Farwell GW, Grootes PM, Schmidt FH. 1992. Radiocarbon AMS dating of pollen extracted from peat samples. Radiocarbon 34:550–556.

Brown TA, Nelson DE, Vogel JS, Southon JR. 1988. Improved collagen extraction by modified Longin method. Radiocarbon 30(2):171–177.

Dean NE. 1988. Geochemistry and archaeological geology of the Carrara Marble, Carrara, Italy. In: Herz N, Waelkens M, editors. Classical marble: Geochemistry, technology, trade. Springer. p. 315–323.

De La Torre HAM, Reyes AV, Zazula GD, Froese DG, Jensen BJ, Southon JR. 2019. Permafrost-preserved wood and bone: Radiocarbon blanks from Yukon and Alaska. Nuclear Instruments and Methods in Physics Research Section B: Beam Interactions with Materials and Atoms 455:154–157.

Deloitte Access Economics. 2013. Economic value of groundwater in Australia. Sydney.

DeNiro MJ. 1985. Postmortem preservation and alteration of in vivo bone collagen isotope ratios in relation to palaeodietary reconstruction. Nature 317(6040):806–809.

DeNiro MJ, Weiner S. 1988. Chemical, enzymatic and spectroscopic characterization of "collagen" and other organic fractions from prehistoric bones. Geochimica et Cosmochimica Acta 52(9):2197–2206.

Dougherty AJ, Thomas ZA, Fogwill C, Hogg A, Palmer J, Rainsley E, Williams AN, Ulm S, Rogers K, Jones BG et al. 2019. Redating the earliest evidence of the mid-Holocene relative sea-level highstand in Australia and implications for global sea-level rise. PLOS ONE 14(7): e0218430.

Douglass K, Cooper J. 2020. Archaeology, environmental justice, and climate change on islands of the Caribbean and Southwestern Indian Ocean. Proceedings of the National Academy of Sciences 117(15):8254–8262.

Dutta K. 2016. Sun, ocean, nuclear bombs, and fossil fuels: Radiocarbon variations and implications for high-resolution dating. Annual Review of Earth and Planetary Sciences 44(1):239–275.

Fogwill CJ, Turney CSM, Menviel L, Baker A, Weber ME, Ellis B, Thomas ZA, Golledge NR, Etheridge D, Rubino M et al. 2020. Southern Ocean carbon sink enhanced by sea-ice feedbacks at the Antarctic Cold Reversal. Nature Geoscience.

Forbes M, Cohen T, Jacobs Z, Marx S, Barber E, Dodson J, Zamora A, Cadd H, Francke A, Constantine M et al. 2021. Comparing interglacials in eastern Australia: A multi-proxy investigation of a new sedimentary record. Quaternary Science Reviews 252:106750, doi: 10.1016/j.quascirev.2020.106750.

Friedlingstein P, Jones MW, O'Sullivan M, Andrew RM, Hauck J, Peters GP, Peters W, Pongratz J, Sitch S, Le Quéré C et al. 2019. Global carbon budget 2019. Earth Syst Sci Data 11(4): 1783–1838.

Friedlingstein P, Meinshausen M, Arora VK, Jones CD, Anav A, Liddicoat SK, Knutti R. 2013. Uncertainties in CMIP5 climate projections due to carbon cycle feedbacks. Journal of Climate 27(2):511–526.

Fu B, Gasser T, Li B, Tao S, Ciais P, Piao S, Balkanski Y, Li W, Yin T, Han L et al. 2020. Short-lived climate forcers have long-term climate impacts via the carbon–climate feedback. Nature Climate Change 10(9):851–855.

Graham PW, Baker A, Andersen MS. 2015. Dissolved organic carbon mobilisation in a groundwater system stressed by pumping. Sci Rep. 5:18487.

Guiry EJ, Staniforth M, Nehlich O, Grimes V, Smith C, Harpley B, Noël S, Richards MP. 2015. Tracing historical animal husbandry, meat trade, and food provisioning: A multi-isotopic approach to the analysis of shipwreck faunal remains from the William Salthouse, Port Phillip, Australia. Journal of Archaeological Science: Reports 1:21–28.

Haghipour N, Ausín B, Usman MO, Ishikawa N, Wacker L, Welte C, Ueda K, Eglinton TI. 2019. Compound-specific radiocarbon analysis by elemental analyzer–accelerator mass spectrometry: Precision and limitations. Analytical Chemistry 91(3):2042–2049.

Haines HA, Gadd PS, Palmer J, Olley JM, Hua Q, Heijnis H. 2018. A new method for dating tree-rings in trees with faint, indeterminate ring boundaries using the ITRAX core scanner. Palaeogeography, Palaeoclimatology, Palaeoecology 497:234–243.

Hedges JI, Ertel JR, Quay PD, Grootes PM, Richey JE, Devol AH, Farwell GW, Schmidt FW, Salati E. 1986. Organic carbon-14 in the Amazon River system. Science 231(4742):1129–1131.

Hogg A, Southon J, Turney C, Palmer J, Bronk Ramsey C, Fenwick P, Boswijk G, Friedrich M, Helle G, Hughen K et al. 2016a. Punctuated shutdown of Atlantic Meridional Overturning Circulation during the Greenland Stadial 1. Sci Rep. 6:25902, doi: 10.1038/srep 25902.

Hogg A, Southon J, Turney C, Palmer J, Ramsey CB, Fenwick P, Boswijk G, Büntgen U, Friedrich M, Helle G et al. 2016b. Decadally resolved Lateglacial radiocarbon evidence from New Zealand kauri. Radiocarbon 58(4):709–733.

Hogg AG, Fifield LK, Turney CSM, Palmer JG, Galbraith R, Baillie MGK. 2006. Dating ancient wood by high-sensitivity liquid scintillation counting and accelerator mass spectrometry-pushing the boundaries. Quaternary Geochronology 1(4):241–248.

Hogg AG, Heaton TJ, Hua Q, Palmer JG, Turney CSM, Southon J, Bayliss A, Blackwell PG, Boswijk G, Bronk Ramsey C et al. 2020. SHCal20 Southern Hemisphere calibration, 0–55,000 years cal BP. Radiocarbon 62(4): 759–778.

Howarth JD, Fitzsimons SJ, Jacobsen GE, Vandergoes MJ, Norris RJ. 2013. Identifying a reliable target fraction for radiocarbon dating sedimentary records from lakes. Quaternary Geochronology 17:68–80.

IPCC. 2018. Global warming of 1.5°C. An IPCC special report on the impacts of global warming of 1.5°C above pre-industrial levels and related global greenhouse gas emission pathways, in the context of strengthening the global response to the threat of climate change, sustainable development, and efforts to eradicate poverty. Intergovernmental Panel on Climate Change.

Knowles TD, Monaghan PS, Evershed RP. 2019. Radiocarbon sample preparation procedures and the first status report from the Bristol Radiocarbon AMS (BRAMS) facility. Radiocarbon 61(5):1541–1550.

Kromer B, Lindauer S, Synal H-A, Wacker L. 2013. MAMS – a new AMS facility at the Curt-Engelhorn-Centre for Archaeometry, Mannheim, Germany. Nuclear Instruments and Methods in Physics Research Section B: Beam Interactions with Materials and Atoms 294:11–13.

Le Clercq M, Van Der Plicht J, Gröning M. 1997. New ^{14}C reference materials with activities of 15 and 50 PMC. Radiocarbon 40(1):295–297.

Le Quéré C, Andres RJ, Boden T, Conway T, Houghton RA, House JI, Marland G, Peters GP, van der Werf GR, Ahlström A et al. 2013. The global carbon budget 1959–2011. Earth Syst Sci Data 5(1):165–185.

Lewis SL, Maslin MA. 2015. Defining the anthropocene. Nature 519(7542):171–180.

Longin R. 1971. New method of collagen extraction for radiocarbon dating. Nature 230: 241–242.

Lowe JJ, Walker MJC. 2000. Radiocarbon dating the last glacial interglacial transition (ca. 14-9 ^{14}C ka BP) in terrestrial and marine records: The need for new quality assurance protocols. Radiocarbon 42:53–68.

Macphail M, Cantrill DJ. 2006. Age and implications of the Forest Bed, Falkland Islands, southwest Atlantic Ocean: Evidence from fossil pollen and spores. Palaeogeography, Palaeoclimatology, Palaeoecology 240(3–4):602–629.

Marra MJ, Alloway BV, Newnham RM. 2006. Paleoenvironmental reconstruction of a well-preserved Stage 7 forest sequence catastrophically buried by basaltic eruptive deposits, northern New Zealand. Quaternary Science Reviews 25:2143–2161.

McDonough LK, Santos IR, Andersen MS, O'Carroll DM, Rutlidge H, Meredith K, Oudone P, Bridgeman J, Gooddy DC, Sorensen JPR et al. 2020. Changes in global groundwater organic carbon driven by climate change and urbanization. Nature Communications. 11(1): 1279.

McIntyre CP, Wacker L, Haghipour N, Blattmann TM, Fahrni S, Usman M, Eglinton TI, Synal H-A. 2017. Online ^{13}C and ^{14}C gas measurements by EA-IRMS–AMS at ETH Zürich. Radiocarbon 59(3):893–903.

Němec M, Wacker L, Hajdas I, Gäggeler H. 2010. Alternative methods for cellulose preparation for AMS measurement. Radiocarbon 52(3): 1358–1370.

O'Connell JF, Allen J, Williams MAJ, Williams AN, Turney CSM, Spooner NA, Kamminga J,

Brown G, Cooper A. 2018. When did *Homo sapiens* first reach Southeast Asia and Sahul? Proceedings of the National Academy of Sciences 115(34):8482–8490.

Palmer JG, Turney CSM, Cook ER, Fenwick P, Thomas Z, Helle G, Jones R, Clement A, Hogg A, Southon J et al. 2016. Changes in El Niño-Southern Oscillation (ENSO) conditions during the Greenland Stadial 1 (GS-1) chronozone revealed by New Zealand tree-rings. Quaternary Science Reviews 153:139–155.

Randerson JT, Lindsay K, Munoz E, Fu W, Moore JK, Hoffman FM, Mahowald NM, Doney SC. 2015. Multicentury changes in ocean and land contributions to the climate-carbon feedback. Global Biogeochem Cycles. 29(6):744–759.

Rasberry SD. 1999. Standard reference material 4990C oxalic acid. National Institute of Standards and Technology.

Reimer PJ, Austin WEN, Bard E, Bayliss A, Blackwell PG, Bronk Ramsey C, Butzin M, Cheng H, Edwards RL, Friedrich M et al. 2020. The IntCal20 Northern Hemisphere radiocarbon age calibration curve (0–55 cal kbp). Radiocarbon 62(4):725–757.

Rockman M, Hritz C. 2020. Expanding use of archaeology in climate change response by changing its social environment. Proceedings of the National Academy of Sciences. 117(15): 8295–8302.

Rozanski K. 1991. Report on consultants' group meeting on ^{14}C reference materials for radiocarbon laboratories. February 18–20, 1991, Vienna. Austria. Internal Report, IAEA, Vienna.

Ruff M, Fahrni S, Gäggeler H, Hajdas I, Suter M, Synal H, Szidat S, Wacker L. 2010. On-line radiocarbon measurements of small samples using elemental analyzer and MICADAS gas ion source. Radiocarbon 52(4):1645–1656.

Sillen A, Parkington J. 1996. Diagenesis of bones from Eland's Bay Cave. Journal of Archaeological Science 23(4):535–542.

Sookdeo A, Kromer B, Büntgen U, Friedrich M, Friedrich R, Helle G, Pauly M, Nievergelt D, Reinig F, Treydte K. 2020. Quality dating: A well-defined protocol implemented at ETH for high-precision ^{14}C-dates tested on late glacial wood. Radiocarbon 62(4):891–899.

Sookdeo A, Wacker L, Fahrni S, McIntyre CP, Friedrich M, Reinig F, Nievergelt D, Tegel W, Kromer B, Büntgen U. 2017. Speed dating: A rapid way to determine the radiocarbon age of wood by EA-AMS. Radiocarbon 59(3): 933–939.

Southwell-Keely P. 2020. The School of Chemistry, University of New South Wales, Sydney: Megacity Design.

Staniforth MJ. 1997. The wreck of the William Salthouse: The earliest attempt to establish trade relations between Canada and Australia.

International Council of Canadian Studies and Carleton University Press.

Steffen W, Broadgate W, Deutsch L, Gaffney O, Ludwig C. 2015. The trajectory of the Anthropocene: The Great Acceleration. The Anthropocene Review. 2(1):81–98.

Steffen W, Richardson K, Rockström J, Schellnhuber HJ, Dube OP, Dutreuil S, Lenton TM, Lubchenco J. 2020. The emergence and evolution of Earth System Science. Nature Reviews Earth & Environment. 1(1):54–63.

Steffen W, Rockström J, Richardson K, Lenton TM, Folke C, Liverman D, Summerhayes CP, Barnosky AD, Cornell SE, Crucifix M et al. 2018. Trajectories of the Earth system in the Anthropocene. Proceedings of the National Academy of Sciences. 115(33):8252–8259.

Strunk A, Olsen J, Sanei H, Rudra A, Larsen NK. 2020. Improving the reliability of bulk sediment radiocarbon dating. Quaternary Science Reviews 242:106442.

Suter M, Müller A, Alfimov V, Christl M, Schulze-König T, Kubik P, Synal H-A, Vockenhuber C, Wacker L. 2010. Are compact AMS facilities a competitive alternative to larger tandem accelerators? Radiocarbon 52(2): 319–330.

Synal H-A, Stocker M, Suter M. 2007. MICADAS: A new compact radiocarbon AMS system. Nuclear Instruments and Methods in Physics Research Section B: Beam Interactions with Materials and Atoms 259(1):7–13.

Szpak P, Metcalfe JZ, Macdonald RA. 2017. Best practices for calibrating and reporting stable isotope measurements in archaeology. Journal of Archaeological Science: Reports. 13:609–616.

Tennant RK, Jones RT, Brock F, Cook C, Turney CSM, Love J, Lee R. 2013. A new flow cytometry method enabling rapid purification of fossil pollen from terrestrial sediments for AMS radiocarbon dating. Journal of Quaternary Science 28(3):229–236.

Thomas Z, Turney CS, Hogg AG, Williams AN, Fogwill CJ. 2019. Investigating subantarctic ^{14}C ages of different peat components: Site and sample selection for developing robust age models in dynamic landscapes. Radiocarbon 61:1–19.

Thomas ZA. 2016. Using natural archives to detect climate and environmental tipping points in the Earth system. Quaternary Science Reviews 152:60–71.

Treble PC, Baker A, Ayliffe LK, Cohen TJ, Hellstrom JC, Gagan MK, Frisia S, Drysdale RN, Griffiths AD, Borsato A. 2017. Hydroclimate of the Last Glacial Maximum and deglaciation in southern Australia's arid margin interpreted from speleothem records (23–15 ka). Climate of the Past 13(6):667–687.

Turney CSM, Fogwill CJ, Palmer JG, van Sebille E, Thomas Z, McGlone M, Richardson S,

Wilmshurst JM, Fenwick P, Zunz V et al. 2017. Tropical forcing of increased Southern Ocean climate variability revealed by a 140–year subantarctic temperature reconstruction. Climate of the Past 13(3):231–248.

Turney CSM, Hobbs D. 2006. ENSO influence on Holocene Aboriginal populations in Queensland, Australia. J Archaeol Sci. 33: 1744–1748.

Turney CSM, Palmer J, Maslin MA, Hogg A, Fogwill CJ, Southon J, Fenwick P, Helle G, Wilmshurst JM, McGlone M et al. 2018. Global peak in atmospheric radiocarbon provides a potential definition for the onset of the Anthropocene epoch in 1965. Sci Rep. 8(1):3293, doi: 3210.1038/s41598-41018-20970–41595.

Van Klinken GJ. 1999. Bone collagen quality indicators for palaeodietary and radiocarbon measurements. Journal of Archaeological Science 26(6):687–695.

Vandergoes MJ, Prior CA. 2003. AMS dating of pollen concentrates-a methodological study of late Quaternary sediments from South Westland, New Zealand. Radiocarbon 45:479–491.

Varney RM, Chadburn SE, Friedlingstein P, Burke EJ, Koven CD, Hugelius G, Cox PM. 2020. A spatial emergent constraint on the sensitivity of soil carbon turnover to global warming. Nature Communications 11(1):5544.

Wacker L, Bonani G, Friedrich M, Hajdas I, Kromer B, Němec M, Ruff M, Suter M, Synal H, Vockenhuber C. 2010a. MICADAS: Routine and high-precision radiocarbon dating. Radiocarbon 52(02):252–262.

Wacker L, Christl M, Synal H-A. 2010b. Bats: A new tool for AMS data reduction. Nuclear Instruments and Methods in Physics Research Section B: Beam Interactions with Materials and Atoms 268(7-8):976–979.

Wacker L, Fahrni SM, Hajdas I, Molnar M, Synal HA, Szidat S, Zhang YL. 2013a. A versatile gas interface for routine radiocarbon analysis with a gas ion source. Nuclear Instruments and Methods in Physics Research Section B: Beam Interactions with Materials and Atoms 294: 315–319.

Wacker L, Fülöp RH, Hajdas I, Molnár M, Rethemeyer J. 2013b. A novel approach to process carbonate samples for radiocarbon measurements with helium carrier gas. Nuclear Instruments and Methods in Physics Research Section B: Beam Interactions with Materials and Atoms 294:214–217.

Wacker L, Němec M, Bourquin J. 2010c. A revolutionary graphitisation system: Fully automated, compact and simple. Nuclear Instruments and Methods in Physics Research B 268(7–8):931–934.

WAIS Divide Project Members. 2015. Precise interpolar phasing of abrupt climate change during the last ice age. Nature 520(7549): 661–665.

Walker M, Lowe J, Blockley SPE, Bryant C, Coombes P, Davies S, Hardiman M, Turney CSM, Watson J. 2012. Lateglacial and early Holocene palaeoenvironmental "events" in Sluggan Bog, Northern Ireland: Comparisons with the Greenland NGRIP GICC05 event stratigraphy. Quaternary Science Reviews 36: 124–138.

Zhang DD, Lee HF, Wang C, Li B, Pei Q, Zhang J, An Y. 2011. The causality analysis of climate change and large-scale human crisis. Proceedings of the National Academy of Sciences 108(42):17296–17301.